Journal of Sound and Vibration (1999) **223**(2), 171–195
Article No. jsvi.1998.1432, available online at http://www.idealibrary.com on IDEAL®

INFLUENCE OF BOUNDARY CONDITIONS ON THE FREQUENCY CHARACTERISTICS OF A ROTATING TRUNCATED CIRCULAR CONICAL SHELL

K. Y. Lam and Li Hua

Department of Mechanical and Production Engineering, National University of Singapore, 10 Kent Ridge Crescent, Singapore 119260

(*Received* 28 *January* 1997, *and in final form* 10 *November* 1997)

The influence of boundary conditions on the frequency characteristics of a rotating conical shell is studied using the Galerkin method. The results obtained include the relationships between the frequency parameter and circumferential wavenumber and between the frequency parameter and rotating velocity at various cone angles under different boundary conditions. The variation of the frequency characteristics at various vibrational modes is also shown. In order to validate the present analysis, several comparisons of the numerical results with those published are made. One comparison is for an infinitely long rotating cylindrical shell; other comparisons are for the non-rotating conical shells. As is expected, these comparisons show very good agreement.

1. INTRODUCTION

There are many engineering applications resulting from studies involving the vibration of rotating shells, such as in the high-speed centrifugal separators, the drive shafts of gas turbines, motors and rotor systems. However, since Bryan [1] discovered the travelling-mode phenomenon in his study of a rotating cylinder, research on rotating shells has been mainly on the vibration of rotating cylindrical shells. Some of the earlier researches were conducted by Di Taranto and Lessen [2], Srinivasan and Lauterbach [3] and Huang and Soedel [4]. Recent studies include the work done by Chun and Bert [5] and Chen *et al*. [6]. The first author, Lam, has also carried out extensive studies on the vibration of both rotating and non-rotating cylindrical shells. He used beam functions to study the effect of boundary conditions on the frequency characteristics for a non-rotating multi-layered cylindrical shell [7], and carried out a comparative study on different thin shell theories for rotating laminated cylindrical shells [8]. He also carried out studies on the rotating laminated composite [9] and rotating sandwich-type cylindrical shells [10]. However, most of the studies on the rotating cylindrical shell were limited to the simply-supported boundary condition. Only a few studies covered other boundary conditions. They included those of Saito and Endo [11],

0022–460X/99/220171 + 25 $30.00/0

Rand and Stavsky [12] and the present authors [13]. By studying a finite length rotating cylindrical shell under different boundary conditions, Saito and Endo [11] found that the boundary conditions have a significant influence on the frequency characteristics of the rotating shell. Rand and Stavsky [12] also studied similar problems. The present authors [13] used a new global approximate numerical technique called as the generalized differential quadrature (GDQ) method to discuss the effects of three boundary conditions on the frequency characteristics of a rotating cylindrical shell.

Although the dynamic behaviour of a rotating cylinder has been studied for over a century, few studies on rotating conical shells have been made. They include the work of the present authors [14] and Sivadas [15]. In reference [14], only simply-supported boundary conditions were considered. The effects of geometric properties of rotating conical shells were presented, including length-to-radius (L/a) and thickness-to-radius (h/a) ratios and so on. However, in both papers, no study on the influence of boundary conditions was made. For non-rotating conical shells, there are many papers discussing the influence of boundary conditions on the frequency characteristics. Earlier studies were conducted by Bacon and Bert [16], Irie *et al*. [17] and Kayran and Vinson [18], while recent studies were carried out by Sivadas and Ganesan [19, 20], Thambiratnam and Zhuge [21] and Tong [22, 23]. For example, Irie *et al*. [17] listed the natural frequencies of isotropic conical shells under nine boundary conditions. Kayran and Vinson [18] studied the frequency characteristics of composite conical shells for eight boundary conditions. Tong [22, 23] also studied a similar problem.

In order to study the influence of boundary conditions on the frequency characteristics of truncated circular rotating conical shells, the present paper presents an approach combining the Galerkin method for the free vibration of rotating conical shells with, respectively, the clamped–clamped (C–C) and simply-supported–simply-supported (S-S) boundary conditions. Having considered the effects of initial hoop tension and centrifugal and coriolis accelerations due to the rotation, this paper focuses on the influence of boundary condition on the relationships between frequency parameter and circumferential wavenumber, and between frequency parameter and rotating velocity. The variations of the frequency characteristics of rotating conical shells at various cone angles, rotating velocities and vibrational modes are also discussed. To examine the accuracy of the present analysis, comparisons are made against the results in the open literature for an infinitely long rotating cylindrical shell and non-rotating conical shells with respectively C–C and S–S boundary conditions. As is shown, very good agreement is obtained.

2. FORMULATIONS

Figure 1 shows the geometry and co-ordinate system for a truncated circular conical shell rotating about its symmetrical and horizontal axis at an angular velocity Ω. In this figure, α is the cone angle, L the length, h the thickness, and a and b are the radii at the two ends. The reference surface of the conical shell is taken to be at its middle surface where an orthogonal co-ordinate system (x, θ, z) is fixed, and $r = r(x)$ is a radius at any co-ordinate point (x, θ, z). The deformations of the rotating conical shell in the meridional x, circumferential θ and normal z directions are defined by u, v and w, respectively.

Using a linear approximation, Chen *et al*. [6] established the general equations for the vibration of a rotating shell of revolution. Based on these equations, by transforming their curvilinear co-ordinate system into the orthogonal co-ordinate systems and then imposing the geometric properties of rotating conical shells on the equations, the governing equations of motion can be derived for a truncated circular rotating conical shell as follows:

$$\frac{\partial N_x}{\partial x} + \frac{1}{r}\frac{\partial N_{x\theta}}{\partial \theta} + \frac{N_\theta^0}{r^2}\left(\frac{\partial^2 u}{\partial \theta^2} - r\cos\alpha\frac{\partial w}{\partial x}\right) + \frac{\sin\alpha}{r}(N_x - N_\theta) + 2\rho h\Omega\sin\alpha\frac{\partial v}{\partial t} - \rho h\frac{\partial^2 u}{\partial t^2} = 0, \quad (1)$$

$$\frac{\partial N_{x\theta}}{\partial x} + \frac{1}{r}\frac{\partial N_\theta}{\partial \theta} + \frac{\cos\alpha}{r}\frac{\partial M_{x\theta}}{\partial x} + \frac{\cos\alpha}{r^2}\frac{\partial M_\theta}{\partial \theta} + \frac{N_\theta^0}{r^2}\left(r\frac{\partial^2 u}{\partial x\,\partial \theta} + \sin\alpha\frac{\partial u}{\partial \theta} + r\sin\alpha\frac{\partial v}{\partial x}\right) + 2\frac{\sin\alpha}{r}N_{x\theta} - 2\rho h\Omega\left(\sin\alpha\frac{\partial u}{\partial t} + \cos\alpha\frac{\partial w}{\partial t}\right) - \rho h\frac{\partial^2 v}{\partial t^2} = 0 \quad (2)$$

$$\frac{\partial^2 M_x}{\partial x^2} + \frac{2}{r}\frac{\partial^2 M_{x\theta}}{\partial \theta\,\partial x} + \frac{1}{r^2}\frac{\partial^2 M_\theta}{\partial \theta^2} + \frac{2\sin\alpha}{r}\frac{\partial M_x}{\partial x} - \frac{\sin\alpha}{r}\frac{\partial M_\theta}{\partial x} + \frac{N_\theta^0}{r^2}\left(\frac{\partial^2 w}{\partial \theta^2} - r\cos\alpha\frac{\partial u}{\partial x}\right) + \frac{N_\theta^0}{r^2}(w\cos^2\alpha + u\sin\alpha\cos\alpha) - \frac{\cos\alpha}{r}N_\theta + 2\rho h\Omega\cos\alpha\frac{\partial v}{\partial t} - \rho h\frac{\partial^2 w}{\partial t^2} = 0. \quad (3)$$

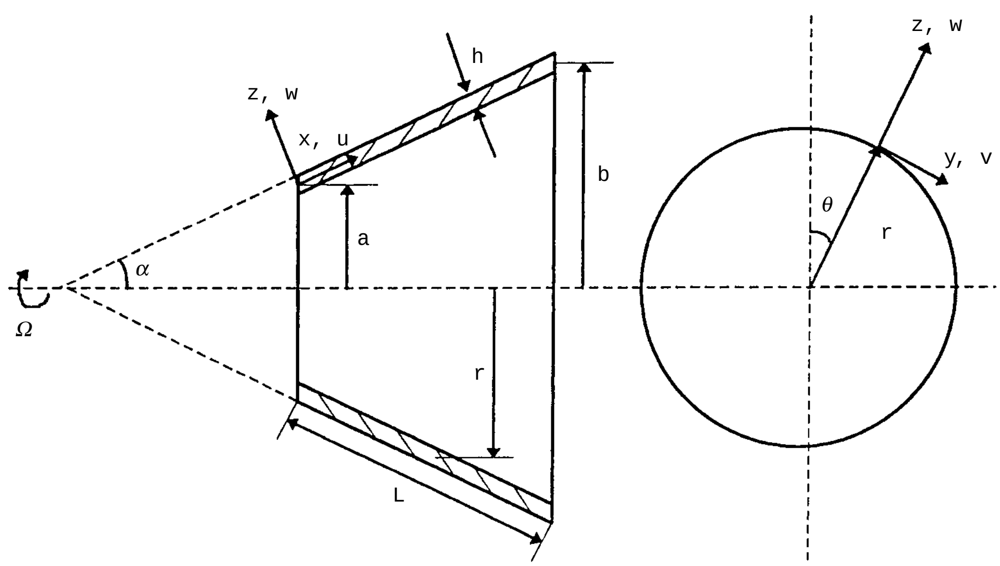

Figure 1. The geometry of a rotating truncated circular conical shell.

TABLE 1

Comparison of frequency parameter $f = \omega b\sqrt{((1-\mu^2)\rho/E}$ *for an infinitely long rotating cylindrical shell* ($m = 1$, $\mu = 0{\cdot}3$, $a/b = 1$, $h/b = 0{\cdot}002$)

Ω (r.p.s.)	n	Chen *et al*. [6]* f_b	Chen *et al*. [6]* f_f	Present results f_b	Present results f_f
0·05	2	0·00167	0·00142	0·00170	0·00145
	3	0·00448	0·00429	0·00450	0·00431
	4	0·00848	0·00833	0·00850	0·00835
	5	0·01370	0·01353	0·01367	0·01355
0·1	2	0·00180	0·00130	0·00189	0·00139
	3	0·00457	0·00419	0·00465	0·00428
	4	0·00855	0·00826	0·00863	0·00834
	5	0·01371	0·01347	0·01379	0·01355

* From equation (45) of Chen *et al*. [6]:

$$f_b = \frac{2n}{n^2+1}\,\Omega + \sqrt{\frac{n^2(n^2-1)^2}{n^2+1}\frac{Eh^2}{\rho(1-\mu^2)12r^2} + \frac{n^4+3}{(n^2+1)^2}\,\Omega^2},$$

$$f_f = \frac{2n}{n^2+1}\,\Omega - \sqrt{\frac{n^2(n^2-1)^2}{n^2+1}\frac{Eh^2}{\rho(1-\mu^2)12r^2} + \frac{n^4+3}{(n^2+1)^2}\,\Omega^2}.$$

Subscripts b and f denote the backward and forward waves, respectively.

Here,

$$\rho = \frac{1}{h}\int_{-h/2}^{h/2} \rho^*(x, \theta, z)\,\mathrm{d}z, \tag{4}$$

TABLE 2

Comparison of frequency parameter $f = \omega b\sqrt{(1-\mu^2)\rho/E}$ *for non-rotating conical shell with S–S boundary condition* ($m = 1$, $\mu = 0{\cdot}3$, $h/b = 0{\cdot}01$, $L \sin\alpha/b = 0{\cdot}25$)

n	$\alpha = 30^\circ$ Present	$\alpha = 30^\circ$ Irie [16]	$\alpha = 45^\circ$ Present	$\alpha = 45^\circ$ Irie [16]	$\alpha = 60^\circ$ Present	$\alpha = 60^\circ$ Irie [16]
2	0·8420	0·7910	0·7655	0·6879	0·6348	0·5722
3	0·7376	0·7284	0·7212	0·6973	0·6238	0·6001
4	0·6362	0·6352	0·6739	0·6664	0·6145	0·6054
5	0·5528	0·5531	0·6323	0·6304	0·6111	0·6077
6	0·4950	0·4949	0·6035	0·6032	0·6171	0·6159
7	0·4661	0·4653	0·5921	0·5918	0·6350	0·6343
8	0·4660	0·4654	0·6001	0·5992	0·6660	0·6650
9	0·4916	0·4892	0·6273	0·6257	0·7101	0·7084

TABLE 3

Comparison of frequency parameter $f=\omega b\sqrt{(1-\mu^2)\rho/E}$ for non-rotating conical shell with C–C boundary condition ($m=1$, $\mu=0{\cdot}3$, $h/b=0{\cdot}01$, $L\sin\alpha/b=0{\cdot}5$)

	$\alpha=45^\circ$		$\alpha=60^\circ$	
n	Present	Irie [16]	Present	Irie [16]
1	0·8452	0·8120	0·6449	0·6316
2	0·6803	0·6696	0·5568	0·5523
3	0·5553	0·5430	0·4818	0·4785
4	0·4778	0·4570	0·4361	0·4298
5	0·4395	0·4095	0·4202	0·4093

$$r=r(x)=a+x\sin\alpha, \tag{5}$$

$$N_\theta^0=\rho h\Omega^2 r^2=\rho h\Omega^2(a+x\sin\alpha)^2, \tag{6}$$

where $\rho^*(x,y,z)$ is the density at any point and ρ is the average density in the z direction at any point; N_θ^0 is defined as the initial hoop tension because of the centrifugal force effect; $\mathbf{N}^T=\{N_x, N_\theta, N_{x\theta}\}$ and $\mathbf{M}^T=\{M_x, M_\theta, M_{x\theta}\}$ are the force and moment vectors and can be obtained from the following general constitutive relationship of a conical shell,

$$\begin{Bmatrix}\mathbf{N}\\ \mathbf{M}\end{Bmatrix}=\begin{bmatrix}\mathbf{A} & \mathbf{B}\\ \mathbf{B} & \mathbf{D}\end{bmatrix}\begin{Bmatrix}\mathbf{e}\\ \mathbf{k}\end{Bmatrix}, \tag{7}$$

where $\mathbf{A}=[A_{ij}]$, $\mathbf{B}=[B_{ij}]$ and $\mathbf{D}=[D_{ij}]$ $(i,j=1,2,6)$ are tensile, coupling and bending stiffness matrixes; $\mathbf{e}^T=\{e_1, e_2, e_{12}\}$ and $\mathbf{k}^T=\{\kappa_1,\kappa_2,\kappa_{12}\}$ (the subscripts 1 and 2 denote the meridional and circumferential directions) are the strain vector and the curvature vector of the reference surface, respectively. The strain and curvature at the reference surface can be defined by the following geometric relationship for the deformations of the reference surface,

$$\begin{gathered}
e_1=\frac{\partial u}{\partial x}\\
e_2=\frac{1}{r(x)}\frac{\partial v}{\partial\theta}+\frac{u\sin\alpha+w\cos\alpha}{r(x)}\\
e_{12}=\frac{1}{r(x)}\frac{\partial u}{\partial\theta}+\frac{\partial v}{\partial x}-\frac{v\sin\alpha}{r(x)}\\
\kappa_1=-\frac{\partial^2 w}{\partial x^2}\\
\kappa_2=-\frac{1}{r^2(x)}\frac{\partial^2 w}{\partial\theta^2}+\frac{\cos\alpha}{r^2(x)}\frac{\partial v}{\partial\theta}-\frac{\sin\alpha}{r(x)}\frac{\partial w}{\partial x}\\
\kappa_{12}=2\left(-\frac{1}{r(x)}\frac{\partial^2 w}{\partial x\,\partial\theta}+\frac{\sin\alpha}{r^2(x)}\frac{\partial w}{\partial\theta}+\frac{\cos\alpha}{r(x)}\frac{\partial v}{\partial x}-\frac{v\sin\alpha\cos\alpha}{r^2(x)}\right).
\end{gathered} \tag{8}$$

Substituting equations (8) into equation (7) and then substituting the resulting equation into governing equations (1)–(3), a set of partial differential governing equations expressed by the displacements u, v and w can be derived as follows:

$$L_{11}u + L_{12}v + L_{13}w = 0,$$
$$L_{21}u + L_{22}v + L_{23}w = 0,$$
$$L_{31}u + L_{32}v + L_{33}w = 0, \tag{9}$$

where L_{ij} $(i, j = 1, 2, 3)$ are the differential operators and are given in the Appendix.

If $\alpha = 0$ and $r(x) = a = b$ are taken into equation (9), the governing equations for the motion of a rotating conical shell are transformed into the equations for

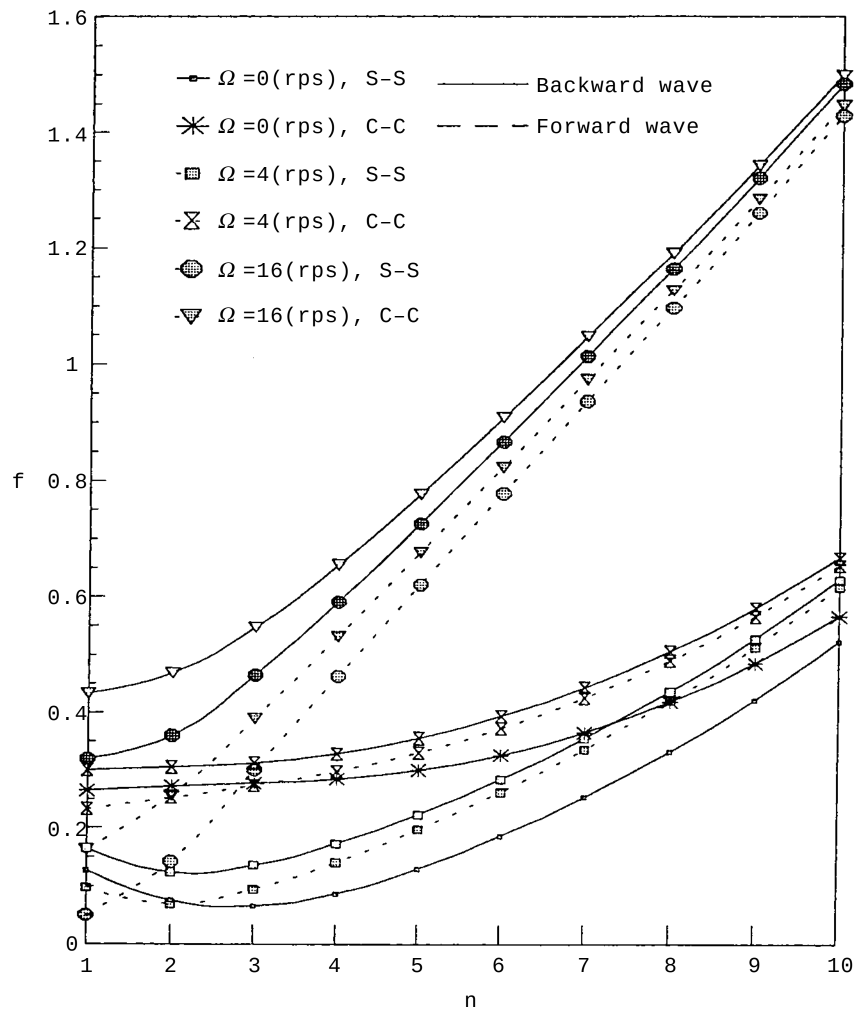

Figure 2. Variation of the frequency parameter f with the circumferential wavenumber n for cone angle $\alpha = 5°$ ($m = 1$, $\mu = 0{\cdot}3$, $h/a = 0{\cdot}02$, $L/a = 20$). Ω (r.p.s.): —⊟—, 0 (S–S); —∗—, 0 (C–C); —⊡—, 4 (S–S); —⧖—, 4 (C–C); —⬡—, 16 (S–S); —▽—, 16 (C–C). —— Backward wave; – – –, forward wave.

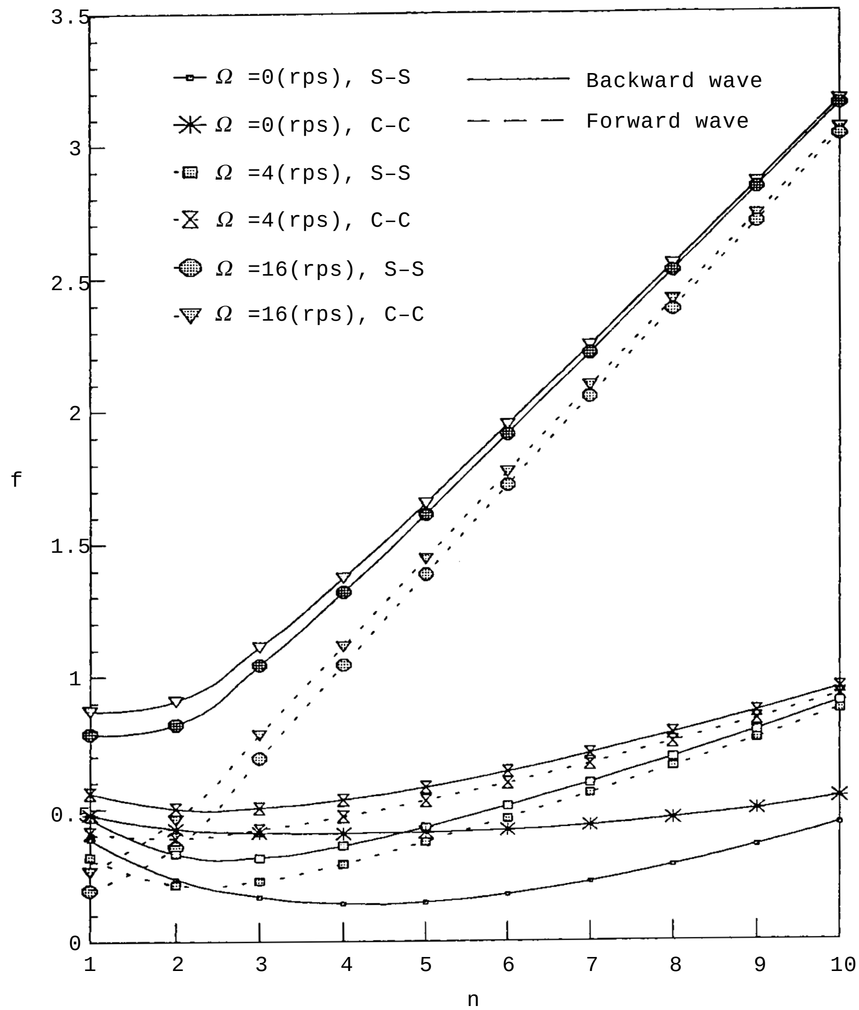

Figure 3. Variation of the frequency parameter f with the circumferential wavenumber n for cone angle $\alpha = 15°$ ($m = 1$, $\mu = 0{\cdot}3$, $h/a = 0{\cdot}02$, $L/a = 20$). Ω (r.p.s.): —⊟—, 0 (S–S); —∗—, 0 (C–C); —⊡—, 4 (S–S); —⧗—, 4 (C–C); —⊙—, 16 (S–S); —▽—, 16 (C–C). —— Backward wave; – – –, forward wave.

the rotating cylindrical shell. The transformations show that the expression of L_{ij} ($i, j = 1, 2, 3$) for the rotating conical shell is much more complicated than that of a rotating cylindrical shell. It should also be noted that L_{ij} of the rotating conical shell is a differential operator with variable coefficients and thus is a function of the co-ordinate variable x, while L_{ij} of a rotating cylindrical shell is a differential operator with constant coefficients and thus is unrelated to variable x.

In addition, for the case of a rotating cylindrical shell, by using some simple trial functions such as equations (16) (see later), the eigensolution can be obtained directly [10]. For the case of a rotating conical shell, however, when using a similar function, the governing equations must be worked out first with approximate approaches such as the Galerkin method before the eigensolution is obtained. The above descriptions are the main differences between the vibrational analyses of the rotating conical and cylindrical shells. They are also the main reasons why the vibrational analysis of a rotating conical shell is much more difficult and complicated than that of a rotating cylindrical shell.

If $\Omega = 0$ is taken into equations (9), the governing equations for the motion of a rotating conical shell are transformed into the equations for the non-rotating conical shell. Substituting the trial function into the resulting governing equations and then performing the approximation process, the eigenvalue equation of the non-rotating conical shell can be obtained and simplified as

$$\left(\omega^2\begin{bmatrix} R_{11} & 0 & 0 \\ 0 & R_{22} & 0 \\ 0 & 0 & R_{33}\end{bmatrix} + \begin{bmatrix} T_{11} & T_{12} & T_{13} \\ T_{21} & T_{22} & T_{23} \\ T_{31} & T_{32} & T_{33}\end{bmatrix}\right)\begin{Bmatrix} U \\ V \\ W \end{Bmatrix} = \begin{Bmatrix} 0 \\ 0 \\ 0 \end{Bmatrix}, \tag{10}$$

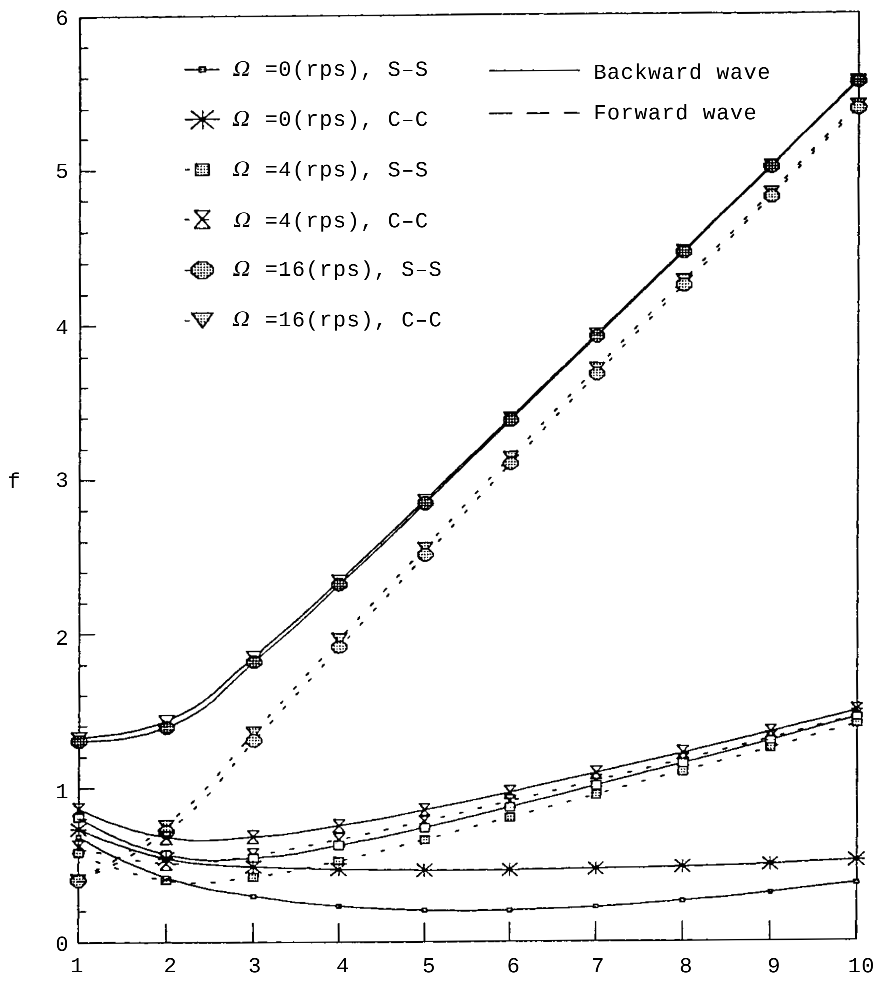

Figure 4. Variation of the frequency parameter f with the circumferential wavenumber n for cone angle $\alpha = 30°$ ($m = 1$, $\mu = 0{\cdot}3$, $h/a = 0{\cdot}02$, $L/a = 20$). Ω (r.p.s.): —⊟—, 0 (S–S); —∗—, 0 (C–C); —⊡—, 4 (S–S); —⧗—, 4 (C–C); —⬡—, 16 (S–S); —▽—, 16 (C–C). —— Backward wave; – – –, forward wave.

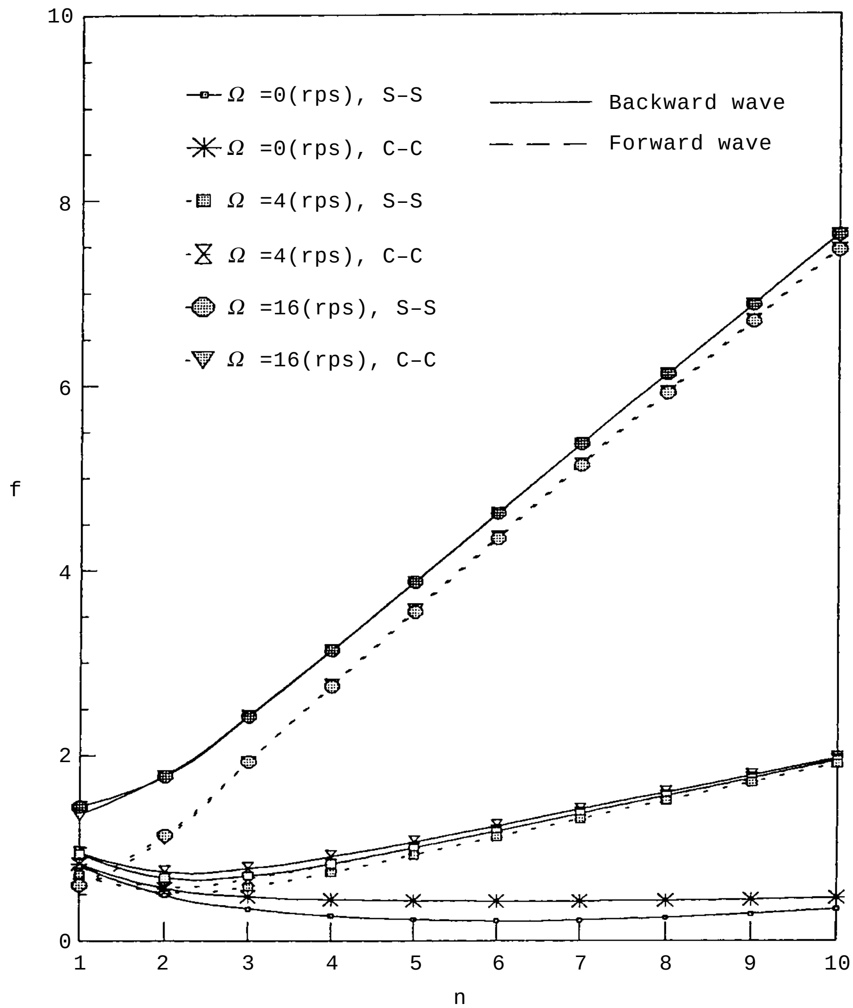

Figure 5. Variation of the frequency parameter f with the circumferential wavenumber n for cone angle $\alpha = 45^\circ$ ($m = 1$, $\mu = 0{\cdot}3$, $h/a = 0{\cdot}02$, $L/a = 20$). Ω (r.p.s.): —□—, 0 (S–S); —∗—, 0 (C–C); —⊡—, 4 (S–S); —⧖—, 4 (C–C); —⬡—, 16 (S–S); —▽—, 16 (C–C). —— Backward wave; – – –, forward wave.

where ω (rad/s) is the natural circular frequency of the present conical shell; U, V and W are the functions of vibrational modes as shown in later equations (13) and (16); and R_{ii} and T_{ij} are the coefficients in terms of the material elastic constants and geometric parameters. Equation (10) is a standard eigenvalue equation so that the eigensolution of free vibration for non-rotating conical shells can be obtained directly by a general eigenvalue approach.

However, for the rotating conical shell, after substituting the same trial function into the governing equation and using similar approximation process, the eigenvalue equation can be derived and simplified as

$$\left(\omega^2\begin{bmatrix} R_{11} & 0 & 0 \\ 0 & R_{22} & 0 \\ 0 & 0 & R_{33}\end{bmatrix} + \omega\begin{bmatrix} S_{11} & S_{12} & S_{13} \\ S_{21} & S_{22} & S_{23} \\ S_{31} & S_{32} & S_{33}\end{bmatrix} + \begin{bmatrix} T_{11} & T_{12} & T_{13} \\ T_{21} & T_{22} & T_{23} \\ T_{31} & T_{32} & T_{33}\end{bmatrix}\right)\begin{Bmatrix} U \\ V \\ W \end{Bmatrix} = \begin{Bmatrix} 0 \\ 0 \\ 0 \end{Bmatrix}, \quad (11)$$

where R_{ii}, T_{ij}, S_{ij} are also similar coefficients expressed by the material elastic constants and geometric parameters. As shown in equation (11), it is a non-standard eigenvalue equation; hence the eigensolution of a rotating conical shell cannot be obtained directly unless some transformations are performed mathematically. This is the main difference and the main implementation problem between the vibrational analyses of rotating and non-rotating conical shells.

So far the derivation of the partial differential governing equations (9) is general and hence it can be used for the dynamic analysis of a rotating truncated circular conical shell with arbitrary boundary conditions. In this paper, however, only isotropic conical shells with respectively C–C and S–S boundary conditions are considered.

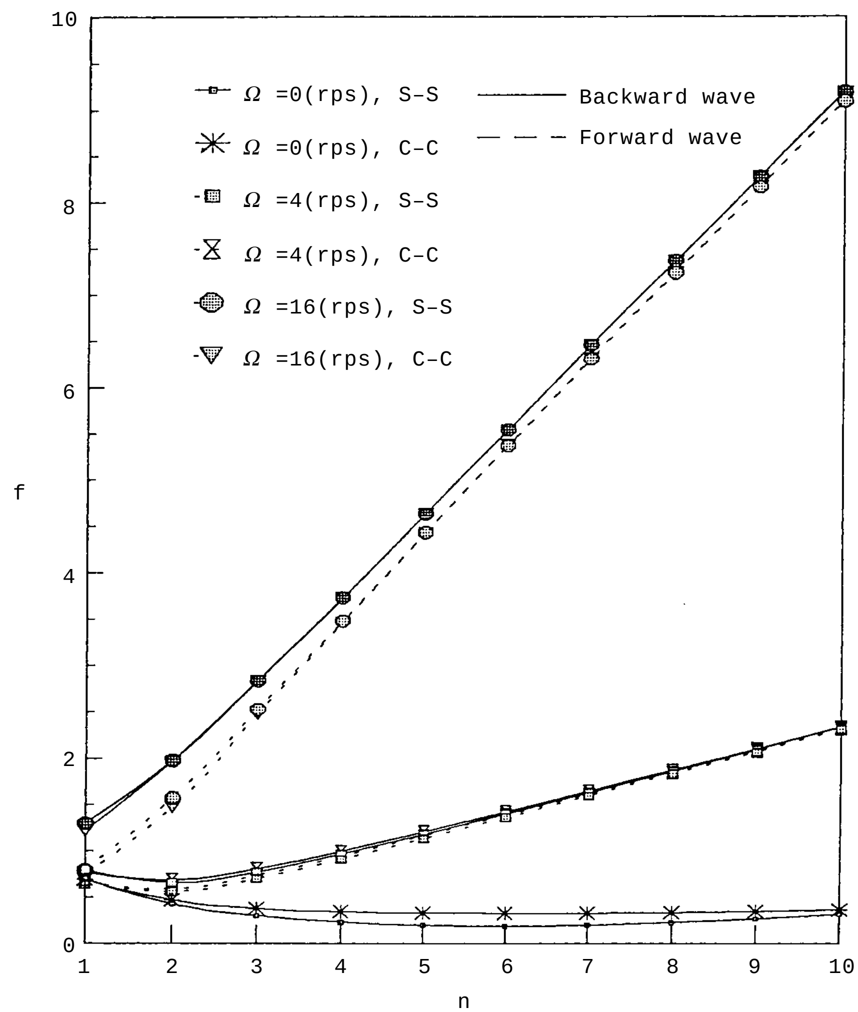

Figure 6. Variation of the frequency parameter f with the circumferential wavenumber n for cone angle $\alpha = 60°$ ($m = 1$, $\mu = 0{\cdot}3$, $h/a = 0{\cdot}02$, $L/a = 20$). Ω (r.p.s.): —⊟—, 0 (S–S); —∗—, 0 (C–C); —⊡—, 4 (S–S); —⧖—, 4 (C–C); —⊙—, 16 (S–S); —▽—, 16 (C–C). —— Backward wave; – – –, forward wave.

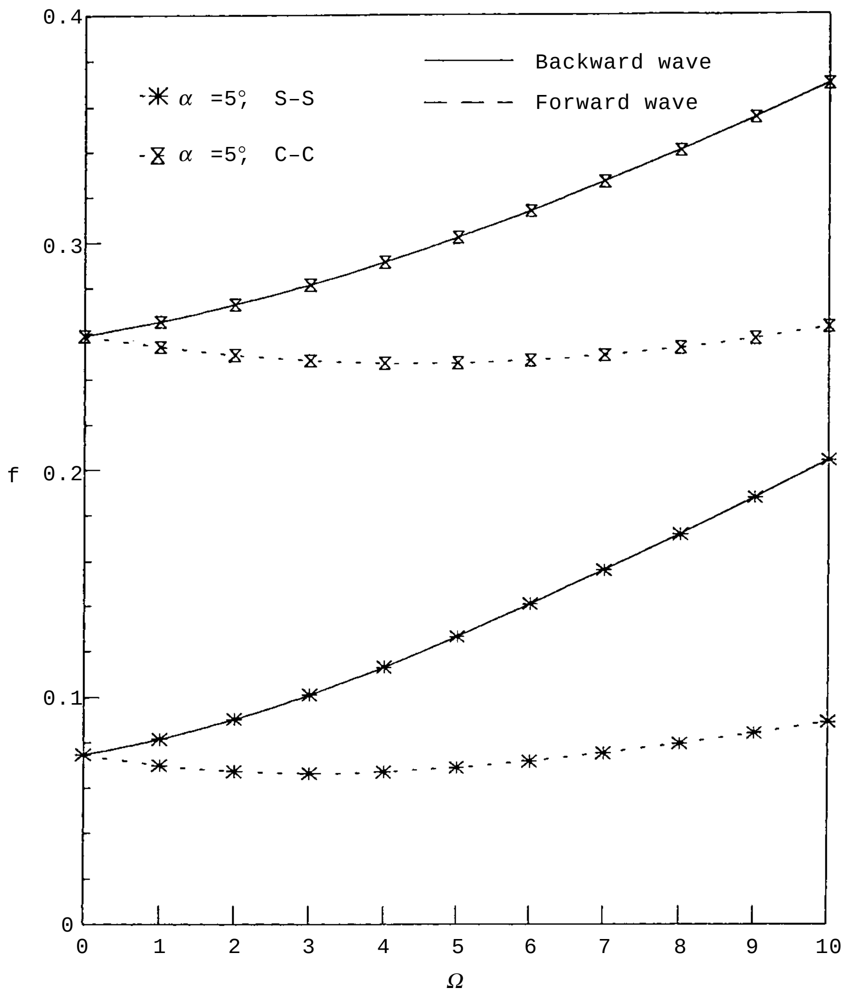

Figure 7. Variation of the frequency parameter f with the rotating velocity Ω (r.p.s.) for cone angle $\alpha = 5^\circ$ ($m = 1$, $n = 2$, $\mu = 0{\cdot}3$, $h/a = 0{\cdot}01$, $L/a = 15$). —∗—, $\alpha = 5^\circ$ (S–S); —⧖—, $\alpha = 5^\circ$, (C–C). ——, Backward wave; – – –, forward wave.

For the clamped boundary condition at both ends (C–C), namely,

$$u = 0, \qquad v = 0, \qquad w = 0, \qquad \frac{\partial w}{\partial x} = 0, \qquad \text{at } x = 0, L, \tag{12}$$

the displacement field can be taken as

$$u = U \sin\left(\frac{m\pi x}{L}\right)\cos(n\theta + \omega t), \qquad v = V \sin\left(\frac{m\pi x}{L}\right)\sin(n\theta + \omega t).$$

$$w = W\left(\sinh\left(\frac{\lambda_m x}{L}\right) - \sin\left(\frac{\lambda_m x}{L}\right) + \gamma_m\left(\cosh\left(\frac{\lambda_m x}{L}\right) - \cos\left(\frac{\lambda_m x}{L}\right)\right)\right)\cos(n\theta + \omega t). \tag{13}$$

Here λ_m and γ_m should satisfy the following conditions

$$\cos\lambda_m \cdot \cosh\lambda_m = 1, \qquad \gamma_m = \frac{\sinh\lambda_m - \sin\lambda_m}{\cos\lambda_m - \cosh\lambda_m} \qquad (m = 1, 2, \ldots). \tag{14}$$

For the following simply-supported boundary condition at both ends (S–S):

$$v = 0, \qquad w = 0, \qquad N_x = 0, \qquad M_x = 0 \qquad \text{at } x = 0, \qquad L, \tag{15}$$

and hence the displacement field can be taken as

$$u = U\cos\left(\frac{m\pi x}{L}\right)\cos(n\theta + \omega t), \quad v = V\sin\left(\frac{m\pi x}{L}\right)\sin(n\theta + \omega t),$$

$$w = W\sin\left(\frac{m\pi x}{L}\right)\cos(n\theta + \omega t). \tag{16}$$

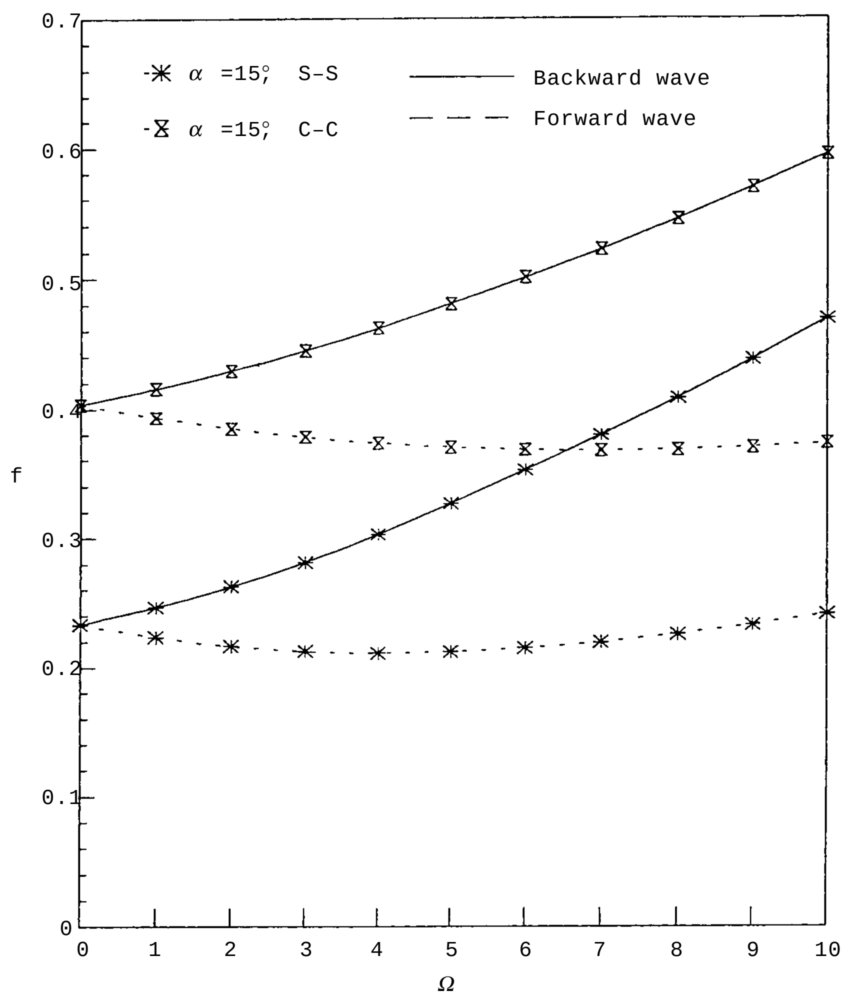

Figure 8. Variation of the frequency parameter f with the rotating velocity Ω (r.p.s.) for cone angle $\alpha = 15°$ ($m = 1$, $n = 2$, $\mu = 0{\cdot}3$, $h/a = 0{\cdot}01$, $L/a = 15$). —∗—, $\alpha = 15°$ (S–S); —⧖—, $\alpha = 15°$ (C–C). ——, Backward wave; – – –, forward wave.

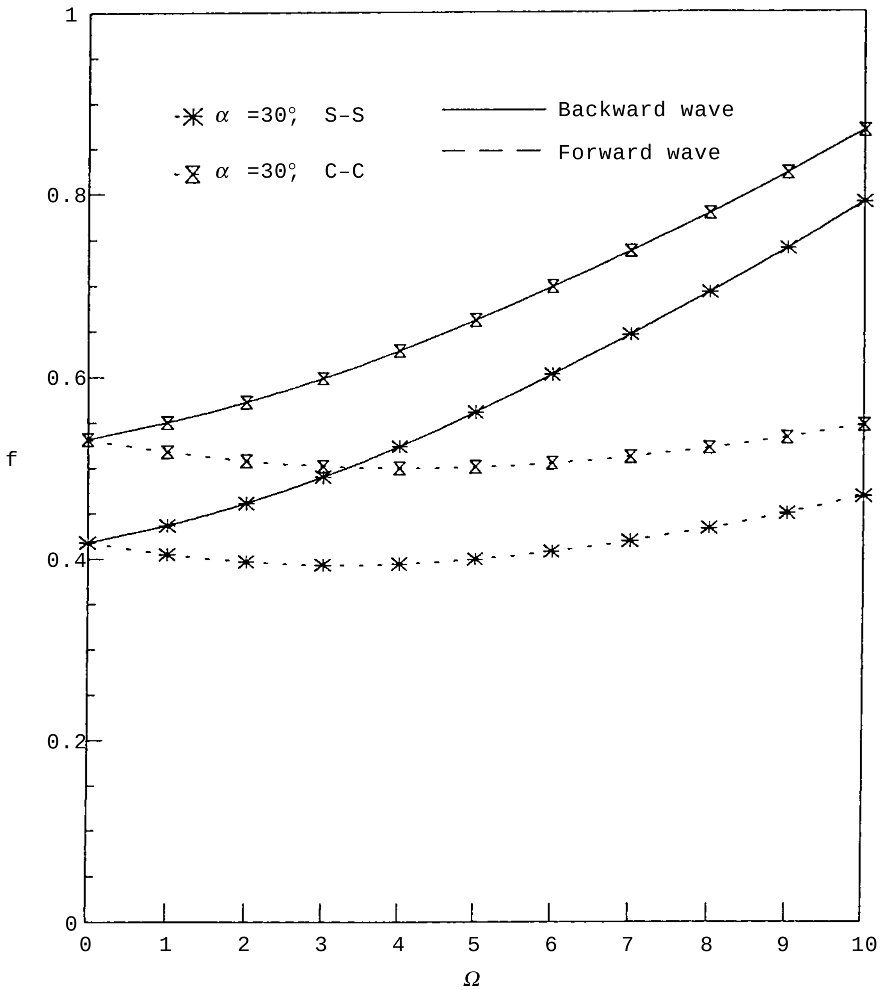

Figure 9. Variation of the frequency parameter f with the rotating velocity Ω (r.p.s.) for cone angle $\alpha = 30^\circ$ ($m = 1$, $n = 2$, $\mu = 0{\cdot}3$, $h/a = 0{\cdot}01$, $L/a = 15$). —∗—, $\alpha=30^\circ$ (S–S); —⧖—, $\alpha=30^\circ$ (C–C). ——, Backward wave; – – –, forward wave.

In equations (13) and (16), ω (rad/s) is the natural circular frequency of the present rotating conical shell, and m and n are the integers representing respectively the meridional and circumferential wave numbers of the rotating shell.

Obviously, the trial functions given by equations (13) can satisfy accurately all the C–C boundary conditions given by equations (12). The trial functions given by equations (16) satisfy accurately the geometric boundary conditions but satisfy only approximately the force boundary conditions in the S–S boundary conditions given by equations (15). However, as the comparisons in Tables 2 and 3 have been shown, the error due to the approximation is acceptable. Moreover, the trial functions given by equations (13) and (16) are simple in form and convenient in implementation; hence they are useful for the present complicated partial differential governing equations.

As is described above, since the governing equations (9) are a set of partial differential equations with variable coefficients, they cannot be solved analytically. Instead, the present paper uses the Galerkin method to obtain an approximate solution. For governing equations (9), the weighted-integral statement of the Galerkin method can be expressed as follows:

$$\int_t \int_\theta \int_x (L_{11}u + L_{12}v + L_{13}w)\delta u \, \mathrm{d}x \, \mathrm{d}\theta \, \mathrm{d}t = 0,$$

$$\int_t \int_\theta \int_x (L_{21}u + L_{22}v + L_{23}w)\delta v \, \mathrm{d}x \, \mathrm{d}\theta \, \mathrm{d}t = 0,$$

$$\int_t \int_\theta \int_x (L_{31}u + L_{32}v + L_{33}w)\delta w \, \mathrm{d}x \, \mathrm{d}\theta \, \mathrm{d}t = 0. \tag{17}$$

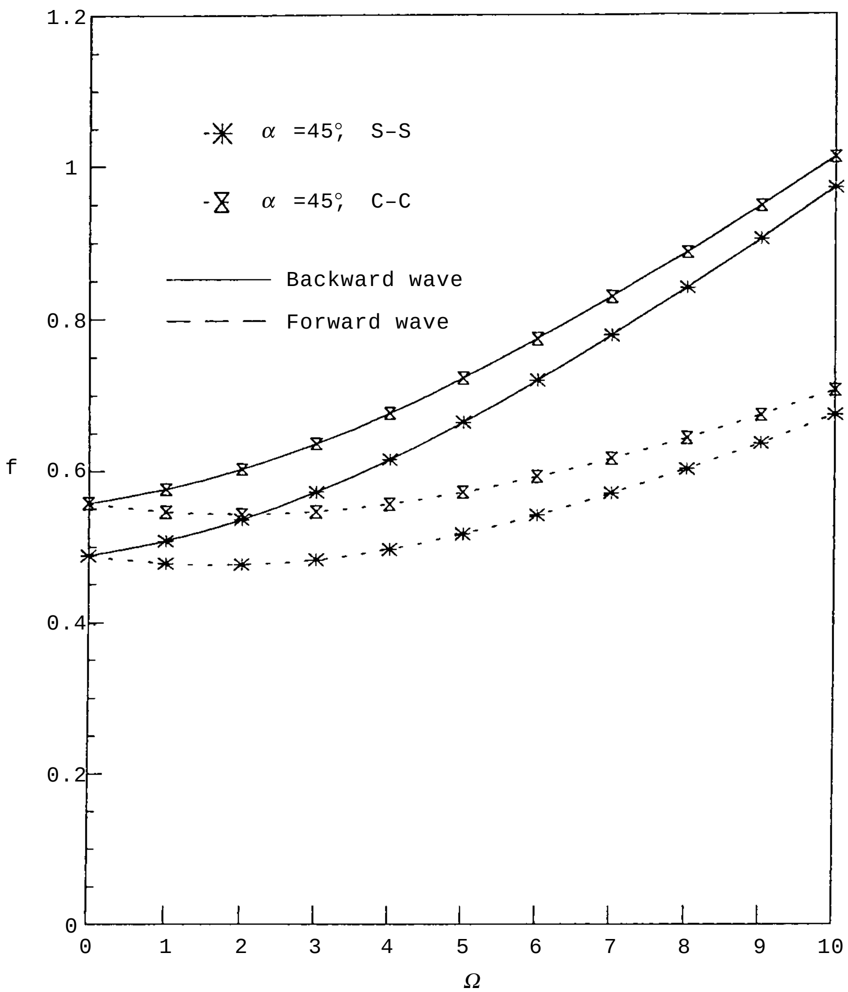

Figure 10. Variation of the frequency parameter f with the rotating velocity Ω (r.p.s.) for cone angle $\alpha = 45°$ ($m = 1$, $n = 2$, $\mu = 0{\cdot}3$, $h/a = 0{\cdot}01$, $L/a = 15$). —∗—, $\alpha = 45°$ (S–S); —⧖—, $\alpha = 45°$ (C–C). ——, Backward wave; – – –, forward wave.

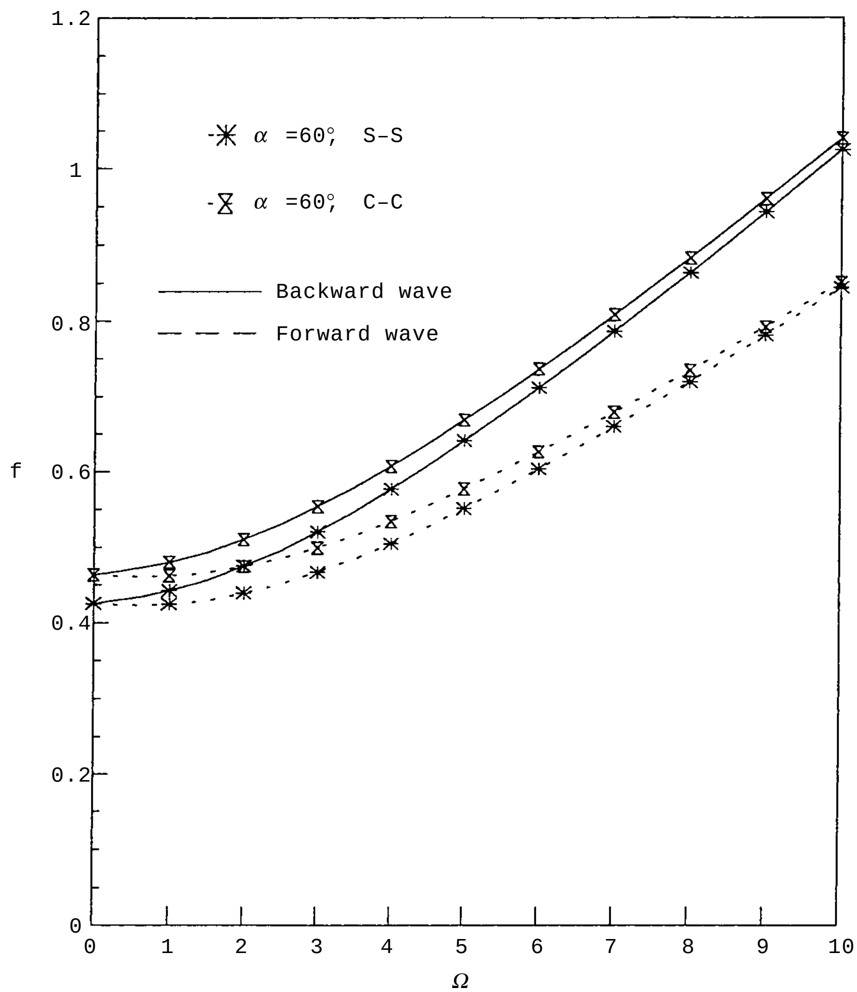

Figure 11. Variation of the frequency parameter f with the rotating velocity Ω (r.p.s.) for cone angle $\alpha = 60^\circ$ ($m = 1$, $n = 2$, $\mu = 0{\cdot}3$, $h/a = 0{\cdot}01$, $L/a = 15$). —∗—, $\alpha = 60^\circ$ (S–S); —⧖—, $\alpha = 60^\circ$ (C–C). ——, Backward wave; – – –, forward wave.

Substituting the trial functions given by equations (13) or (16) into the weighted-integral statement given by equations (17) depending on the boundary condition, the eigenvalue equation of the rotating conical shell is obtained in the following matrix form:

$$\begin{bmatrix} C_{11} & C_{12} & C_{13} \\ C_{21} & C_{22} & C_{23} \\ C_{31} & C_{32} & C_{33} \end{bmatrix} \begin{Bmatrix} U \\ V \\ W \end{Bmatrix} = \begin{Bmatrix} 0 \\ 0 \\ 0 \end{Bmatrix}. \tag{18}$$

Here the coefficients C_{ij} $(i, j = 1, 2, 3)$ are very complicated and are long expressions in terms of frequency, material elastic constant and geometric parameter. One example of this, namely, C_{11} can be found in Lam *et al*. [14] by using the trial functions (16) for the S–S boundary condition.

Eigenvalue equation (18) may be solved by imposing the non-trivial condition and then setting the determinant of the characteristic matrix equal to zero, namely,

$$\begin{vmatrix} C_{11} & C_{12} & C_{13} \\ C_{21} & C_{22} & C_{23} \\ C_{31} & C_{32} & C_{33} \end{vmatrix} = 0. \tag{19}$$

Expanding the determinant (19), a polynomial equation of ω is obtained

$$d_0\omega^6 + d_1\omega^5 + d_2\omega^4 + d_3\omega^3 + d_4\omega^2 + d_5\omega + d_6 = 0, \tag{20}$$

where d_i ($i = 0, 1, 2, \ldots, 6$) are constants. The six roots in equation (20) can be solved by using the Newton–Raphson procedure. The two roots for which the absolute values are the smallest are the eigensolutions discussed. A bifurcation phenomenon exists in the present vibrational analysis. Namely, for the

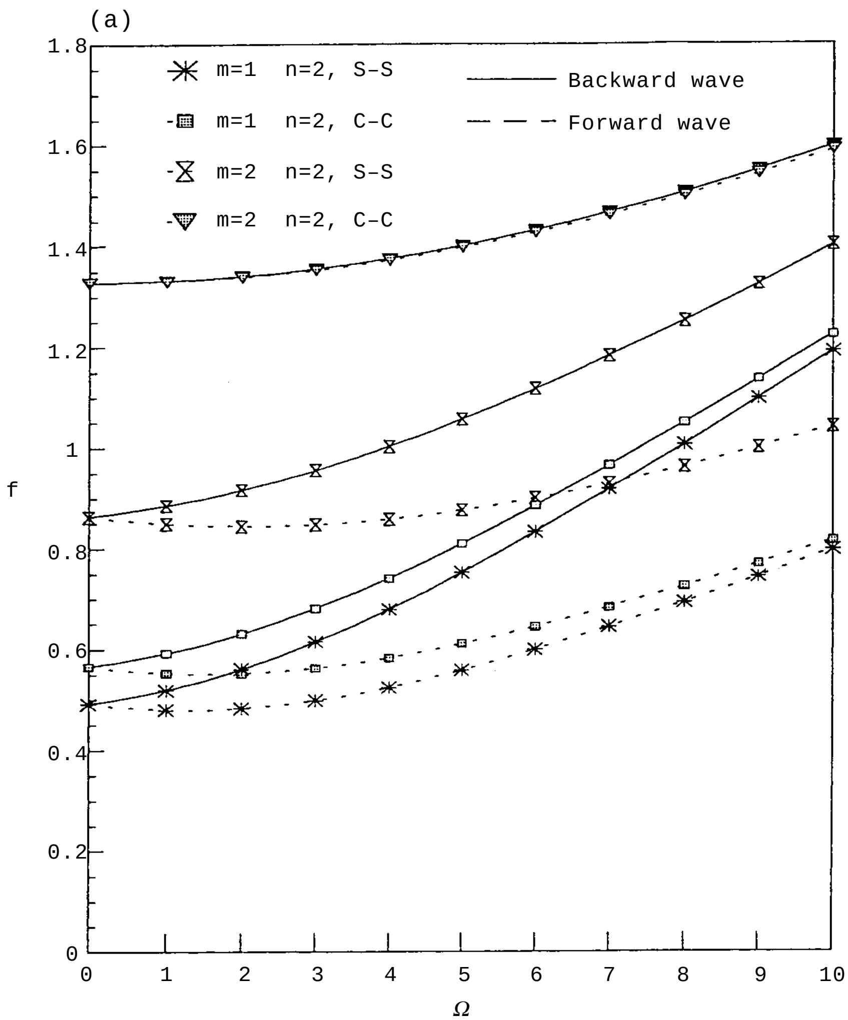

Fig. 12(a).

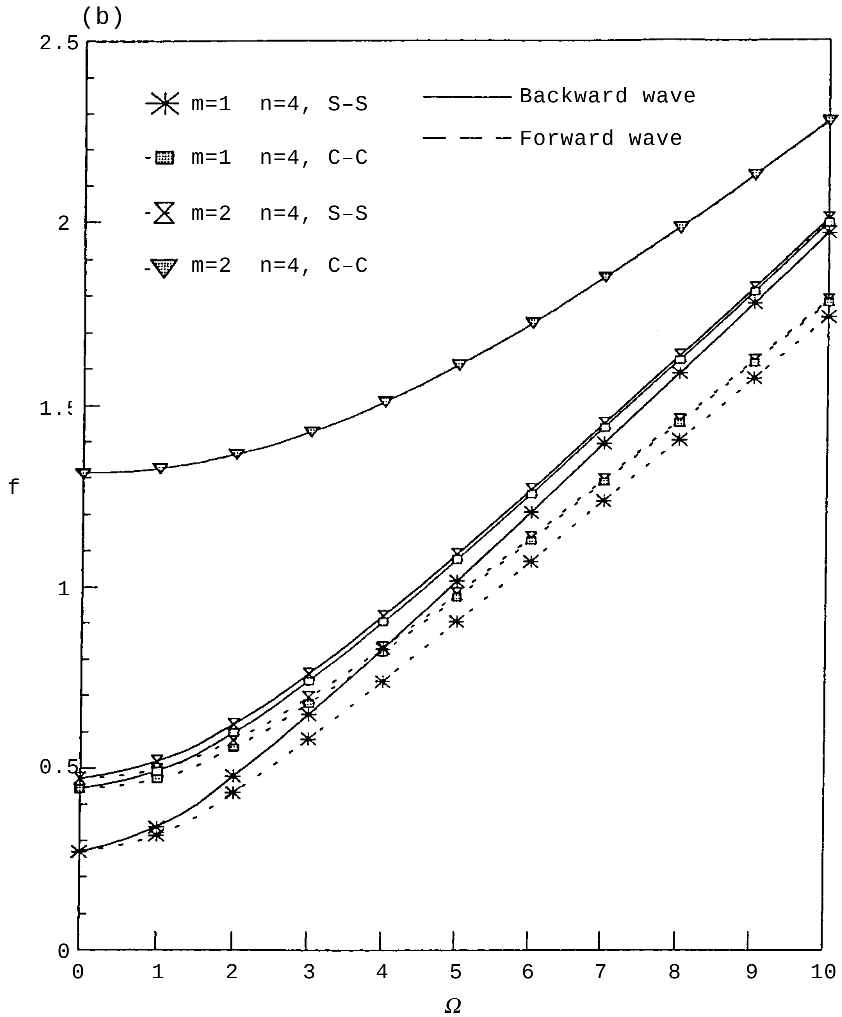

Fig. 12(b).

Figure 12. Variation of the frequency parameter f with the rotating velocity Ω (r.p.s.) at various vibrational modes ($\mu = 0{\cdot}3$, $\alpha = 45°$, $h/a = 0{\cdot}02$, $L/a = 20$). (a) —∗—, $m=1$, $n=2$ (S–S); —⊡—, $m=1$, $n=2$ (C–C); —⧖—, $m=2$, $n=2$ (S–S); —▽—, $m=2$, $n=2$ (C–C). (b) —∗—, $m=1$, $n=4$ (S–S); —⊡—, $m=1$, $n=4$ (C–C); —⧖—, $m=2$, $n=4$ (S–S); —▽—, $m=2$, $n=4$ (C–C). ——, Backward wave; – – –, forward wave.

non-rotating conical shell, these two eigenvalues are identical; for the rotating conical shell, they are real numbers, one positive and other negative. They correspond respectively to the backward and forward travelling waves or to the positive and negative rotating velocities.

3. RESULTS AND DISCUSSION

To examine the accuracy of the present analysis, three comparisons are made against the results in the open literature. The first comparison, as shown in Table 1, is for an infinitely long rotating cylindrical shell by taking $\alpha = 0$ into the present formulations. The second, as shown in Table 2, is for a non-rotating conical shell with S–S boundary condition by taking $\Omega = 0$ into the present formulations. The third, as shown in Table 3, is for a non-rotating conical shell with C–C boundary condition by taking $\Omega = 0$, similarly. For ease of comparison and discussion, a non-dimensional frequency parameter is defined as follows:

$$f = \omega b\sqrt{\frac{(1-\mu^2)\rho}{E}}\,. \tag{21}$$

The above three comparisons show very good agreement between the present computed results and those in the open literature and thus indicate the accuracy of the present work.

In the present discussion on the influence of the boundary conditions on frequency characteristics, three studies were presented for the free vibration of rotating truncated circular conical shells. The first, as shown in Figures 2–6, studies the influence of boundary conditions on the relationship between the frequency parameter f and the circumferential wavenumber n at various rotating velocities. The second, as shown in Figures 7–11, studies the influence of boundary conditions on the relationship between the frequency parameter f and the rotating velocity Ω for various cone angles. The third, as shown in Figures 12(a) and (b), studies the influence of boundary conditions on frequency characteristics at various vibrational modes.

In the figures, the backward wave is represented by a solid line and the forward wave by a dashed line; the unit for the rotating velocity Ω is r.p.s. (revolutions per second or Hz). The results are presented for the clamped boundary condition at both ends (C–C) and simply-supported boundary condition at both ends (S–S).

Taking the geometric properties $h/a = 0{\cdot}02$ and $L/a = 20$, Figures 2–6 show the variations of the frequency parameter f against the circumferential wavenumber n for the free vibration of the rotating truncated circular conical shells under the C–C and S–S boundary conditions. These five figures correspond to the five different cone angles, namely, $\alpha = 5^\circ$, 15°, 30°, 45° and 60°, and at three different rotating velocities, $\Omega = 0$, 4 and 16 r.p.s. For the case of the non-rotating conical shell, i.e., $\Omega = 0$, it can be seen from the figures that there is a significant difference between the frequency parameters of small cone angles corresponding to the C–C and S–S boundary conditions; this difference decreases with increasing cone angle. For the case of the rotating conical shell, it should be noted that similar results also occur. The frequency parameter f increases with increasing rotating velocity Ω for the given circumferential wavenumber n; the frequency parameter f also increases with increasing circumferential wavenumber n at a given rotating velocity Ω. It should also be noted that, as the circumferential wavenumber n increases, the difference of the frequency parameters between the C–C and S–S boundary conditions decreases for the given rotating velocity Ω; the difference also decreases with increasing rotating velocity Ω for a given circumferential wavenumber n. Therefore, it can be concluded that there is an influence of the boundary conditions on the relationship between the frequency parameter f and circumferential wavenumber n. This influence becomes significant for the small cone angle, or small circumferential wavenumber n or low rotating velocity. However, as circumferential wavenumber n or the cone angle α increases, such influence tends to become insignificant for the given rotating velocity.

Taking the geometric properties $h/a = 0{\cdot}01$, $L/a = 15$ and circumferential wavenumber $n = 2$, Figures 7–11 show the variation of the frequency parameter f against the rotating velocity Ω for the free vibration of the rotating truncated circular conical shells with the C–C and S–S boundary conditions. These five figures correspond to the five different cone angles, namely, $\alpha = 5$, 15, 30, 45 and 60°. From these figures, it can be seen that the frequency parameter f increases with an increase in rotating velocity Ω for both C–C and S–S boundary conditions. The difference of the frequency parameters between the C–C and S–S boundary conditions is also larger for the smaller cone angle, while as the cone angle increases, the difference becomes small. Therefore, it can be concluded that boundary conditions have a significant effect on the relationship between frequency parameter f and rotating velocity Ω; this influence is significant when the cone angle of the conical shell is small. However, with the increase of the cone angle, the influence will become insigificant.

Taking the geometric properties $h/a = 0{\cdot}02$, $L/a = 20$ and the cone angle $\alpha = 45^{\circ}$, Figure 12(a) and (b) show the variations of the frequency parameter f against the rotating velocity Ω at various vibrational modes (m, n) for the C–C and S–S rotating conical shells, where m and n are the meridional and circumferential wavenumbers. From the two figures, it can be seen that the difference of the frequency parameters between the C–C and S–S boundary conditions for mode (2, 2) is much larger than that of mode (1, 2). Similarly, the difference of the frequency parameters for mode (2, 4) is also much larger than that of mode (1, 4). In addition, it should be noted that for the S–S boundary condition, the absolute value of the frequency parameter f of the backward wave is always larger than that of the forward wave. The difference of frequency parameters between the backward and forward waves generally increases with an increasing rotating velocity Ω. However, for the C–C boundary conditions, similar trends can only be observed in the low-order vibrational mode such as (1, 2) or (1, 4). In the high-order vibrational mode such as (2, 2), (2, 4) or even higher-order mode, the difference of frequency parameters between backward and forward waves is small and tends to vanish. From the above studies, it can be concluded that the boundary conditions significantly affect the variation of the frequency parameter f against the rotating velocity Ω, and such influence becomes more significant for the higher-order vibrational mode.

4. CONCLUSIONS

Taking into account the initial hoop tension and the centrifugal and coriolis accelerations, the present paper presents a method to study the influence of the boundary conditions on the frequency characteristics of a rotating truncated circular conical shell. The present study is for the rotating isotropic conical shells with the C–C and S–S boundary conditions. The computed results are obtained for the frequency characteristics at various cone angles, rotating velocities and vibrational modes. From the results obtained, it is found that the boundary conditions have an influence on the frequency characteristics of the free vibration for a rotating truncated circular conical shell. Such influence is more significant in the case of a small circumferential wavenumber, or low rotating velocity, or small cone angle or higher-order vibrational mode. However, such influence becomes small for a large circumferential wavenumber, or high rotating speed, or large cone or lower-order vibrational mode. The present numerical formulations and implementations are found to be accurate and reliable when compared with results in the open literature for an infinitely long rotating cylindrical shell and non-rotating isotropic conical shell under C–C and S–S boundary conditions.

REFERENCES

1. G. H. BRYAN 1890 *Proceedings of the Cambridge Philosophical Society* **7**, 101–111. On the beats in the vibration of a revolving cylinder or bell.
2. R. A. DI TARANTO and M. LESSEN 1964 *Journal of Applied Mechanics* **31**, 700–701. Coriolis acceleration effect on the vibration of a rotating thin-walled circular cylinder.
3. A. V. SRINIVASAN and G. F. LAUTERBACH 1971 *Journal of Engineering for Industry* **93**, 1229–1232. Traveling waves in rotating cylindrical shells.
4. S. C. HUANG and W. SOEDEL 1988 *Journal of the Acoustical Society of America* **84**, 275–285. On the forced vibration of simply supported rotating cylindrical shells.
5. D. K. CHUN and C. W. BERT 1993 *Composites Engineering* **3**, 633–643. Critical speed analysis of laminated composite, hollow drive shafts.
6. Y. CHEN, H. B. ZHAO and Z. P. SHEN 1993 *Journal of Sound and Vibration* **160**, 137–160. Vibrations of high speed rotating shells with calculations for cylindrical shells.
7. K. Y. LAM and C. T. LOY 1995 *Journal of Sound and Vibration* **188**, 363–384. Effects of boundary conditions on frequencies of a multi-layered cylindrical shell.
8. K. Y. LAM and C. T. LOY 1995 *Journal of Sound and Vibration* **186**, 23–35. Analysis of rotating laminated cylindrical shells by different thin shell theories.
9. K. Y. LAM and C. T. LOY 1994 *Composites Engineering* **4**, 1153–1167. On vibrations of thin rotating laminated composite cylindrical shells.
10. K. Y. LAM and C. T. LOY 1995 *International Journal of Solids and Structures* **32**, 647–663. Free vibrations of a rotating multi-layered cylindrical shell.
11. T. SAITO and M. ENDO 1986 *Journal of Sound and Vibration* **107**, 17–28. Vibration of finite length, rotating cylindrical shells.
12. O. RAND and Y. STAVSKY 1991 *International Journal of Solids and Structures* **28**, 831–843. Free vibrations of spinning composite cylindrical shells.
13. LI HUA and K. Y. LAM 1998 *International Journal of Mechanical Sciences* **40**, 443–439. Frequency characteristics of a thin rotating cylindrical shell using the generalized differential quadrature method.
14. K. Y. LAM and LI HUA 1997 *International Journal of Solids and Structures* **34**, 2183–2197. Vibrational analysis of a rotating truncated circular conical shell.
15. K. R. SIVADAS 1995 *Journal of Sound and Vibration* **186**, 99–109. Vibration analysis of pre-stressed rotating thick circular conical shell.
16. M. BACON and C. W. BERT 1967 *AIAA Journal* **5**, 413–417. Unsymmetric free vibrations of orthotropic sandwich shells of revolution.
17. T. IRIE, G. YAMADA and K. TANAKA 1984 *Journal of Sound and Vibration* **92**, 447–453. Natural frequencies of truncated conical shells.
18. A. KAYRAN and J. R. VINSON 1990 *AIAA Journal* **28**, 1259–1269. Free vibration analysis of laminated composite truncated circular conical shells.
19. K. R. SIVADAS and N. GANESAN 1991 *Journal of Sound and Vibration* **148**, 477–491. Vibration analysis of laminated conical shells with variable thickness.

20. K. R. SIVADAS and N. GANESAN 1992 *Journal of Sound and Vibration* **152**, 27–37. Vibration analysis of thick composite clamped conical shells of varying thickness.
21. D. P. THAMBIRATNAM and Y. ZHUGE 1993 *Engineering Structure* **15**, 83–89. Axisymmetric free vibration analysis of conical shells.
22. L. Y. TONG 1993 *International Journal of Engineering Sciences* **31**, 719–733. Free vibration of orthotropic conical shells.
23. L. Y. TONG 1993 *International Journal of Mechanical Sciences* **35**, 47–61. Free vibration of composite laminated conical shells.
24. A. E. H. LOVE 1952 *A Treatise on the Mathematical Theory of Elasticity*. Cambridge: Cambridge University Press; fourth edition.

APPENDIX

The differential operators L_{ij} $(i, j = 1, 2, 3)$ defined in equations (9) can be written as:

$$L_{11} = -\frac{A_{22}\sin^2\alpha}{r^2(x)} - \rho h\frac{\partial^2}{\partial t^2} + \left(\frac{A_{66}}{r^2(x)} + \Omega^2\rho h\right)\frac{\partial^2}{\partial\theta^2} + \frac{(A_{11} + A_{12} - A_{21})\sin\alpha}{r(x)}\frac{\partial}{\partial x} + \frac{2A_{16}}{r(x)}\frac{\partial^2}{\partial x\,\partial\theta} + A_{11}\frac{\partial^2}{\partial x^2}, \tag{A1}$$

$$\begin{aligned} L_{12} = {} & \frac{2(B_{16} + B_{26})\cos\alpha\sin^2\alpha}{r^3(x)} + \frac{A_{26}\sin^2\alpha}{r^2(x)} + 2\Omega\rho h\sin\alpha\frac{\partial}{\partial t} \\ & - \left(\frac{(B_{12} + B_{22} + 2B_{66})\cos\alpha\sin\alpha}{r^3(x)} + \frac{(A_{22} + A_{66})\sin\alpha}{r^2(x)}\right)\frac{\partial}{\partial\theta} \\ & + \left(\frac{B_{26}\cos\alpha}{r^3(x)} + \frac{A_{26}}{r^2(x)}\right)\frac{\partial^2}{\partial\theta^2} - \left(\frac{2(B_{16} + B_{26})\cos\alpha\sin\alpha}{r^2(x)} + \frac{A_{26}\sin\alpha}{r(x)}\right)\frac{\partial}{\partial x} \\ & + \left(\frac{(B_{12} + 2B_{66})\cos\alpha}{r^2(x)} + \frac{(A_{12} + A_{66})}{r(x)}\right)\frac{\partial^2}{\partial x\,\partial\theta} \\ & + \left(A_{16} + \frac{2B_{16}\cos\alpha}{r(x)}\right)\frac{\partial^2}{\partial x^2}, \end{aligned} \tag{A2}$$

$$\begin{aligned} L_{13} = {} & -\frac{A_{22}\cos\alpha\sin\alpha}{r^2(x)} - \left(\frac{2(B_{16} + B_{26})\sin^2\alpha}{r^3(x)} - \frac{A_{26}\cos\alpha}{r^2(x)}\right)\frac{\partial}{\partial\theta} \\ & + \frac{(B_{12} + B_{22} + 2B_{66})\sin\alpha}{r^3(x)}\frac{\partial^2}{\partial\theta^2} - \frac{B_{26}}{r^3(x)}\frac{\partial^3}{\partial\theta^3} \\ & + \left(\frac{B_{22}\sin^2\alpha}{r^2(x)} + \frac{A_{12}\cos\alpha}{r(x)} - \Omega^2\rho h r(x)\cos\alpha\right)\frac{\partial}{\partial x} \\ & + \frac{(2B_{16} + B_{26})\sin\alpha}{r^2(x)}\frac{\partial^2}{\partial x\,\partial\theta} - \frac{(B_{12} + 2B_{66})}{r^2(x)}\frac{\partial^3}{\partial x\,\partial\theta^2} \\ & - \frac{(B_{11} + B_{12} - B_{21})\sin\alpha}{r(x)}\frac{\partial^2}{\partial x^2} - \frac{3B_{16}}{r(x)}\frac{\partial^3}{\partial x^2\,\partial\theta} - B_{11}\frac{\partial^3}{\partial x^3}, \end{aligned} \tag{A3}$$

$$L_{21} = -\frac{B_{26}\cos\alpha\sin^2\alpha}{r^3(x)} + \frac{A_{26}\sin^2\alpha}{r^2(x)} - 2\Omega\rho h\sin\alpha\frac{\partial}{\partial t}$$

$$+\left(\frac{(B_{22}-B_{66})\cos\alpha\sin\alpha}{r^3(x)} + \frac{(A_{22}+A_{66})\sin\alpha}{r^2(x)} + \Omega^2\rho h\sin\alpha\right)\frac{\partial}{\partial\theta}$$

$$+\left(\frac{B_{26}\cos\alpha}{r^3(x)} + \frac{A_{26}}{r^2(x)}\right)\frac{\partial^2}{\partial\theta^2} + \left(\frac{B_{26}\cos\alpha\sin\alpha}{r^2(x)} + \frac{(2A_{16}+A_{26})\sin\alpha}{r(x)}\right)\frac{\partial}{\partial x}$$

$$+\left(\Omega^2\rho hr(x) + \frac{(B_{21}+B_{66})\cos\alpha}{r^2(x)} + \frac{(A_{21}+A_{66})}{r(x)}\right)\frac{\partial^2}{}$$

$$\times\,\partial x\,\partial\theta + \left(A_{16} + \frac{B_{16}\cos\alpha}{r(x)}\right)\frac{\partial^2}{\partial x^2}, \quad \text{(A4)}$$

$$L_{22} = \frac{4D_{66}\cos^2\alpha\sin^2\alpha}{r^4(x)} + \frac{B_{66}\cos\alpha\sin^2\alpha}{r^3(x)} - \frac{A_{66}\sin^2\alpha}{r^2(x)} - \rho h\frac{\partial^2}{\partial t^2}$$

$$-\left(\frac{4D_{26}\cos^2\alpha\sin\alpha}{r^4(x)} + \frac{4B_{26}\cos\alpha\sin\alpha}{r^3(x)}\right)\frac{\partial}{\partial\theta}$$

$$+\left(\frac{D_{22}\cos^2\alpha}{r^4(x)} + \frac{2B_{22}\cos\alpha}{r^3(x)} + \frac{A_{22}}{r^2(x)}\right)\frac{\partial^2}{\partial\theta^2}$$

$$-\left(\frac{4D_{66}\cos^2\alpha\sin\alpha}{r^3(x)} + \frac{B_{66}\cos\alpha\sin\alpha}{r^2(x)} - \frac{A_{66}\sin\alpha}{r(x)} - \Omega^2\rho hr(x)\sin\alpha\right)\frac{\partial}{\partial x}$$

$$+\left(\frac{3D_{26}\cos^2\alpha}{r^3(x)} + \frac{5B_{26}\cos\alpha}{r^2(x)} + \frac{2A_{26}}{r(x)}\right)\frac{\partial^2}{\partial x\,\partial\theta}$$

$$+\left(\frac{2D_{66}\cos^2\alpha}{r^2(x)} + \frac{3B_{66}\cos\alpha}{r(x)} + A_{66}\right)\frac{\partial^2}{\partial x^2}, \quad \text{(A5)}$$

$$L_{23} = -\frac{B_{26}\cos^2\alpha\sin\alpha}{r^3(x)} + \frac{A_{26}\cos\alpha\sin\alpha}{r^2(x)} - 2\Omega\rho h\cos\alpha\frac{\partial}{\partial t}$$

$$-\left(\frac{4D_{66}\cos\alpha\sin^2\alpha}{r^4(x)} - \frac{B_{22}\cos^2\alpha}{r^3(x)} - \frac{A_{22}\cos\alpha}{r^2(x)}\right)\frac{\partial}{\partial\theta}$$

$$+\left(\frac{4D_{26}\cos\alpha\sin\alpha}{r^4(x)} + \frac{2B_{26}\sin\alpha}{r^3(x)}\right)\frac{\partial^2}{\partial\theta^2} - \left(\frac{D_{22}\cos\alpha}{r^4(x)} + \frac{B_{22}}{r^3(x)}\right)\frac{\partial^3}{\partial\theta^3}$$

$$+\left(\frac{D_{26}\cos\alpha\sin^2\alpha}{r^3(x)} + \frac{B_{26}(\cos^2\alpha - \sin^2\alpha)}{r^2(x)} + \frac{A_{26}\cos\alpha}{r(x)}\right)\frac{\partial}{\partial x}$$

$$-\left(\frac{(D_{22} - 4D_{66})\cos\alpha\sin\alpha}{r^3(x)} + \frac{B_{22}\sin\alpha}{r^2(x)}\right)\frac{\partial^2}{\partial x\,\partial\theta}$$

$$-\left(\frac{3D_{26}\cos\alpha}{r^3(x)} + \frac{3B_{26}}{r^2(x)}\right)\frac{\partial^3}{\partial x\,\partial\theta^2}$$

$$-\left(\frac{D_{26}\cos\alpha\sin\alpha}{r^2(x)} + \frac{(2B_{16} + B_{26})\sin\alpha}{r(x)}\right)\frac{\partial^2}{\partial x^2}$$

$$-\left(\frac{(D_{21} + 2D_{66})\cos\alpha}{r^2(x)} + \frac{(B_{21} + 2B_{66})}{r(x)}\right)\frac{\partial^3}{\partial x^2\,\partial\theta}$$

$$-\left(B_{16} + \frac{D_{16}\cos\alpha}{r(x)}\right)\frac{\partial^3}{\partial x^3}, \tag{A6}$$

$$L_{31} = \frac{B_{22}\sin^3\alpha}{r^3(x)} - \frac{A_{22}\cos\alpha\sin\alpha}{r^2(x)} + \Omega^2\rho h\cos\alpha\sin\alpha$$

$$-\left(\frac{B_{26}\sin^2\alpha}{r^3(x)} + \frac{A_{26}\cos\alpha}{r^2(x)}\right)\frac{\partial}{\partial\theta}$$

$$+\frac{(B_{22} - 2B_{66})\sin\alpha}{r^3(x)}\frac{\partial^2}{\partial\theta^2} + \frac{B_{26}}{r^3(x)}\frac{\partial^3}{\partial\theta^3}$$

$$-\left(\frac{B_{22}\sin^2\alpha}{r^2(x)} + \frac{A_{21}\cos\alpha}{r(x)} + \Omega^2\rho h r(x)\cos\alpha\right)\frac{\partial}{\partial x}$$

$$+\frac{B_{26}\sin\alpha}{r^2(x)}\frac{\partial^2}{\partial x\,\partial\theta} + \frac{(B_{21} + 2B_{66})}{r^2(x)}\frac{\partial^3}{\partial x\,\partial\theta^2}$$

$$+\frac{(2B_{11} + B_{12} - B_{21})\sin\alpha}{r(x)}\frac{\partial^2}{\partial x^2} + \frac{3B_{16}}{r(x)}\frac{\partial^3}{\partial x^2\,\partial\theta} + B_{11}\frac{\partial^3}{\partial x^3}, \tag{A7}$$

$$L_{32} = -\frac{4(D_{16}+D_{26})\cos\alpha\sin^3\alpha}{r^4(x)} + \frac{(2\cos^2\alpha - \sin^2\alpha)B_{26}\sin\alpha}{r^3(x)} + \frac{A_{26}\cos\alpha\sin\alpha}{r^2(x)}$$

$$+ 2\Omega\rho h\cos\alpha\frac{\partial}{\partial t} - \left(\frac{6D_{26}\cos\alpha\sin\alpha}{r^4(x)} + \frac{3B_{26}\sin\alpha}{r^3(x)}\right)\frac{\partial^2}{\partial\theta^2}$$

$$+ \left(\frac{D_{22}\cos\alpha}{r^4(x)} + \frac{B_{22}}{r^3(x)}\right)\frac{\partial^3}{\partial\theta^3}$$

$$+ \left(\frac{(2D_{12}+D_{22}+4D_{66})\cos\alpha\sin^2\alpha}{r^4(x)} + \frac{(\sin^2\alpha - \cos^2\alpha)B_{22} + 2B_{66}\sin^2\alpha}{r^3(x)}\right.$$

$$\left. - \frac{A_{22}\cos\alpha}{r^2(x)}\right)\frac{\partial}{\partial\theta} + \left(\frac{4(D_{16}+D_{26})\cos\alpha\sin^2\alpha}{r^3(x)}\right.$$

$$\left. + \frac{(\sin^2\alpha - 2\cos^2\alpha)B_{26}}{r^2(x)} - \frac{A_{26}\cos\alpha}{r(x)}\right)\frac{\partial}{\partial x}$$

$$- \left(\frac{(2D_{12}+D_{22}+8D_{66})\cos\alpha\sin\alpha}{r^3(x)} + \frac{(B_{22}+2B_{66})\sin\alpha}{r^2(x)}\right)\frac{\partial^2}{\partial x\,\partial\theta}$$

$$+ \left(\frac{4D_{26}\cos\alpha}{r^3(x)} + \frac{3B_{26}}{r^2(x)}\right)\frac{\partial^3}{\partial x\,\partial\theta^2}$$

$$- \left(\frac{2(D_{16}+D_{26})\cos\alpha\sin\alpha}{r^2(x)} + \frac{(B_{26}-B_{16})\sin\alpha}{r(x)}\right)\frac{\partial^2}{\partial x^2}$$

$$+ \left(\frac{(D_{12}+4D_{66})\cos\alpha}{r^2(x)} + \frac{(B_{12}+2B_{66})}{r(x)}\right)\frac{\partial^3}{\partial x^2\,\partial\theta}$$

$$+ \left(B_{16} + \frac{2D_{16}\cos\alpha}{r(x)}\right)\frac{\partial^3}{\partial x^3}, \tag{A8}$$

$$
\begin{aligned}
L_{33} = {} & \frac{B_{22} \cos \alpha \sin^2 \alpha}{r^3(x)} - \frac{A_{22} \cos^2 \alpha}{r^2(x)} + \Omega^2 \rho h \cos^2 \alpha - \rho h \frac{\partial^2}{\partial t^2} \\
& + \left(\frac{4(D_{16} + D_{26}) \sin^3 \alpha}{r^4(x)} \right. \\
& \left. - \frac{4B_{26} \cos \alpha \sin \alpha}{r^3(x)} \right) \frac{\partial}{\partial \theta} + \frac{6D_{26} \sin \alpha}{r^4(x)} \frac{\partial^3}{\partial \theta^3} - \frac{D_{22}}{r^4(x)} \frac{\partial^4}{\partial \theta^4} \\
& - \left(\frac{2(D_{12} + D_{22} + 4D_{66}) \sin^2 \alpha}{r^4(x)} + \frac{2B_{22} \cos \alpha}{r^3(x)} + \Omega^2 \rho h \right) \frac{\partial^2}{\partial \theta^2} - \frac{D_{22} \sin^3 \alpha}{r^3(x)} \frac{\partial}{\partial x} \\
& - \left(\frac{2(2D_{16} + D_{26}) \sin^2 \alpha}{r^3(x)} - \frac{4B_{26} \cos \alpha}{r^2(x)} \right) \frac{\partial^2}{\partial x \, \partial \theta} \\
& + \frac{2(D_{12} + 4D_{66}) \sin \alpha}{r^3(x)} \frac{\partial^3}{\partial x \, \partial \theta^2} \\
& - \frac{4D_{26}}{r^3(x)} \frac{\partial^4}{\partial x \, \partial \theta^3} + \left(\frac{D_{22} \sin^2 \alpha}{r^2(x)} + \frac{(B_{12} + B_{21}) \cos \alpha}{r(x)} \right) \frac{\partial^2}{\partial x^2} \\
& + \frac{2D_{16} \sin \alpha}{r^2(x)} \frac{\partial^3}{\partial x^2 \, \partial \theta} \\
& - \frac{(D_{12} + D_{21} + 4D_{66})}{r^2(x)} \frac{\partial^4}{\partial x^2 \, \partial \theta^2} - \frac{(2D_{11} + D_{12} - D_{21}) \sin \alpha}{r(x)} \frac{\partial^3}{\partial x^3} \\
& - \frac{4D_{16}}{r(x)} \frac{\partial^4}{\partial x^3 \, \partial \theta} - D_{11} \frac{\partial^4}{\partial x^4}.
\end{aligned} \tag{A9}
$$